Renewable Energy 131 (2019) 37–44

Contents lists available at ScienceDirect

Renewable Energy

journal homepage: www.elsevier.com/locate/renene

# A wind farm control strategy for power reserve maximization

Sara Siniscalchi-Minna [a, c, *], Fernando D. Bianchi [b], Mikel De-Prada-Gil [a], Carlos Ocampo-Martinez [c]

[a] Catalonia Institute for Energy Research, IREC, Jardins de le Dones de Negre, s/n, 08930 Barcelona, Spain
[b] CONICET and Instituto Balseiro, Bustillos 9500, S.C. Bariloche, Argentina
[c] Automatic Control Department, Universitat Politècnica de Catalunya, Institut de Robòtica i Informàtica Industrial (CSIC-UPC), Llorens i Artigas, 4-6, 08028 Barcelona, Spain

ARTICLE INFO

*Article history:*
Received 3 January 2018
Received in revised form
16 May 2018
Accepted 29 June 2018
Available online 6 July 2018

*Keywords:*
Frequency control
Wind farm power regulation
De-loading operation
Power reserve maximization

ABSTRACT

Nowadays, in many countries wind energy is responsible for a significant part of the electricity generation. For this reason, Transmission System Operators (TSOs) are now demanding the wind power plants (WPPs) to contribute with ancillary services such as frequency support. To this end, WPPs must be able to temporally increase the active power delivered into the grid to compensate consume and demand imbalances. This implies that WPPs now work below their maximum capacity to keep some power reserve to be able to inject extra power into the grid when needed. This reserve depends on the available wind power, which is directly connected with the wind speed faced by each turbine within the WPP. However, wind speed is negative affected by the wakes caused by the upstream turbines. This paper proposes a control algorithm to distribute the power contribution of each turbine seeking to minimize the wake effects and thus maximize the power reserve. The proposed algorithm is evaluated by simulations for the case of a WPP of 12 wind turbines.



## 1. Introduction

The ever-growing environmental concerns and cost-effectiveness of renewable energy sources (RES), such as wind and solar energies, have led to a significant increase of their penetration levels into the electrical power system. Nowadays, wind power generation supplies more than 10% of the European consumptions and is expected to grow to 33% in 2030 [1]. This increasingly large deployment of RES into the electrical grid has contributed to decrease the dependency on fossil fuels. However, the high penetration of non-synchronous generators replacing conventional power plants, based on synchronous generation, leads to a system inertia reduction and thus affecting power system stability and reliability. RESs, if not properly controlled, inject into the grid highly variable power that may result in significant frequency fluctuations [2]. As a consequence, Transmission System Operators (TSOs) are now requiring wind power plants (WPPs) to participate in the provision of ancillary services, which so far have been relied on conventional sources. Typically, WPPs were operated to maximize the power output with the aim of minimizing wind energy cost. In this new context, the power production should be adjusted according to the TSOs requirements. The development of new wind farm control strategies for supplying automatic and fast response as ancillary service provider is acquiring relevance as a major-focus research topic [3]. There is an increasing interest from grid operators in requiring the WPPs to participate in ancillary services, such as frequency control [4] and voltage support [5].

Depending on the time range, WPP contributions in frequency support can be classified in two groups. WPPs can be used to provide inertial frequency support limiting the rate of fall during the initial instants of a frequency drop. To this end, wind turbines can release within milliseconds the kinetic energy stored in the rotating mass [6]. In order to ensure a more effective inertial frequency support, some authors have proposed optimization procedures to maximize the wind farm power generation and the kinetic energy stored in the turbines [7,8]. WPPs can also provide primary and secondary frequency supports by delivering into the grid additional active power during longer period of time in order to drive the frequency at its nominal setting. To be able to provide this kind of support, WPPs should work in de-loading mode, i.e. below their maximum power production capacity. This implies to keep certain

* Corresponding author. Catalonia Institute for Energy Research, IREC, Jardins de le Dones de Negre, s/n, 08930 Barcelona, Spain.
*E-mail address:* ssiniscalchi@irec.cat (S. Siniscalchi-Minna).

https://doi.org/10.1016/j.renene.2018.06.112

amount of power reserve that can be released in case of frequency drops. Clearly, the larger the power reserve, the more effective the frequency support. Therefore, there is interest in maximize this capability of WPPs as it could bring some cost benefits in case of participation of WPPs in balancing markets [9,10].

The maximum power available in WPPs depends on the wind speed faced by each turbine. Within a wind farm, these wind conditions are imposed by the wakes produced by the upstream turbines [11]. In the literature, several strategies have been proposed to minimize the wake effect in order to maximize total power generation and minimize the power losses caused by the wakes. Some of them are based on redirecting the wakes around the downstream turbines by yawing [12,13] or tilting [14,15] the wind turbines, whereas others seek to redistribute the power contribution of each turbine [16,17]. Further, purposely setting the power contribution of each turbine by decreasing the generation of the upstream turbines has shown potential for minimizing the mechanical loads and thus extending the lifetime of the wind farm [18,19].

In this paper, a wind farm control strategy is proposed to maximize the power reserve during de-loading operation while maintaining the total power delivered by the WPP at the point of common coupling (PCC). The proposed approach aims to determine the power set-points for every turbine considering that commonly wind farms operate in waked conditions. With the goal of maximizing the power reserve, the proposed wind farm control strategy distributes the power contribution of each turbine in order to maximize the available power (i.e., the power reserve). The proposed approach was tested for a wind farm model of 12 wind turbines using a simulator that models the dynamic behavior of the wake effect by using the common dynamic wake meandering model [20].

The remainder of this paper is organized as follows. The wind farm model is presented in Section 2. Section 3 describes the proposed wind farm control strategy. In Section 4, the simulation set-up is presented and the main results are discussed for the wind farm selected as case study. Finally, the conclusions are drawn in Section 5.

## 2. Wind farm modeling

The WPP control scheme under study is shown in Fig. 1. According to the utility demands, the TSO requires the WPP to deliver a power $P_{\text{dem}}$. Depending on the available power $P_{\text{av},i}$, the wind farm central controller sets the power set-points for each turbine $P_{\text{r},i}$ in order that the total generated power $P_{\text{g}}$ matches the demand $P_{\text{dem}}$.

In circumstances with available power higher than the power demand, the wind farm is able to deliver an extra power for helping in primary frequency support. This extra power capability is referred to as the total power reserve and is given, for a wind farm of $N$ turbines, by

$$P_{\text{res}} = P_{\text{av,tot}} - P_{\text{dem}}, \tag{1}$$

where

$$P_{\text{av,tot}} = \sum_{i=1}^{N} P_{\text{av},i}(v_i). \tag{2}$$

and $v_i$ the wind speed experienced by the turbine.

In high wind energy conditions, WPPs are able to meet the total power demanded by the TSO by de-loading some wind turbines. For wind turbines with this capability, the generated power can be expressed as

$$P_{\text{g},i} = \kappa_1 C_{\text{p}}(a_i) v_i^3 = \min\left(\kappa_1 C_{\text{p,max}} v_i^3, P_{\text{r},i}\right), \tag{3}$$

where $\kappa_1 = (\pi\rho R^2/2)$, $\rho$ is the air density, $R$ is the rotor radius, and $C_{\text{p}}$ is the power coefficient. Besides, (3) can be written as a function of the induction factor $a_i$ [21], i.e.

$$C_{\text{p},i} = 4a_i(1 - a_i)^2. \tag{4}$$

In normal operation, the induction factor $a_i$ can be assumed taking values between 0 and 1/3. Therefore, (4) is an increasing function of $a_i$ and the maximum value $C_{\text{p,max}}$ is obtained at $a_i = 1/3$. De-loading operations can be achieved by acting, individually [22] or in simultaneously [23], on both pitch and torque control actions to ensure sub-optimal operational conditions. According to (3), the generated power can be set to a given value $P_{\text{r},i}$ if wind conditions allow. This expression also indicates that, for a given $v_i$, there exists a unique $0 \le a_i \le 1/3$ producing $P_{\text{g},i} = P_{\text{r},i}$. The relationship among $P_{\text{g},i}$, $v_i$ and $a_i$ is shown in Fig. 2.

The available power at each wind turbine, i.e., the maximum generation capacity for the wind conditions $v_i$, is given by

$$P_{\text{av},i} = \min\left(\kappa_1 C_{\text{p,max}} v_i^3, P_{\text{rated}}\right), \tag{5}$$

being $P_{\text{rated}}$ the rated power limit. Fig. 3 shows a generic available power characteristics as a function of the wind speed.

Each turbine within a farm has different reserve capacity as wind conditions depend on the geographical distribution of the wind resources and the air flow disturbances caused by the wake effects induced by up-stream turbines. The wake results from the interaction of the incoming wind speed $v_i$ with the wind turbine rotor, such that the wind speed in the outflow field decreases.

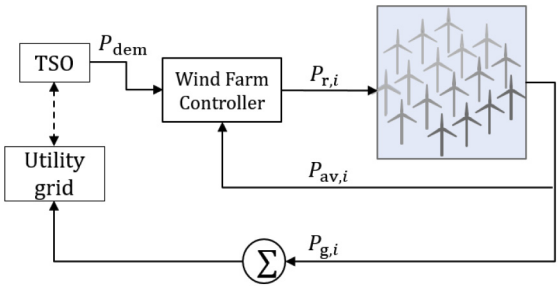


**Fig. 1.** WPP control scheme under study.

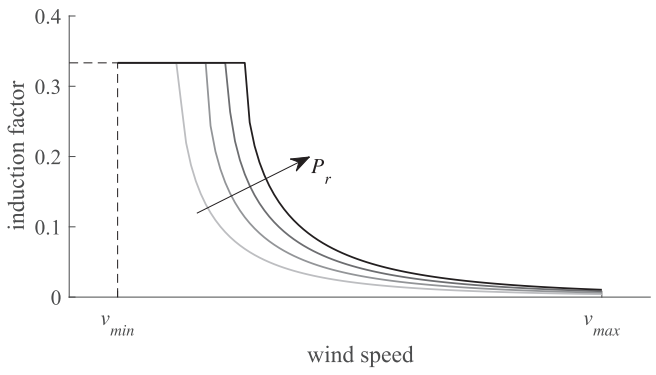


**Fig. 2.** Induction factor $a$ – wind speed $v$ characteristic for several power set-points $P_r$. The black line corresponds to the nominal case ($P_r = P_{\text{rated}}$).

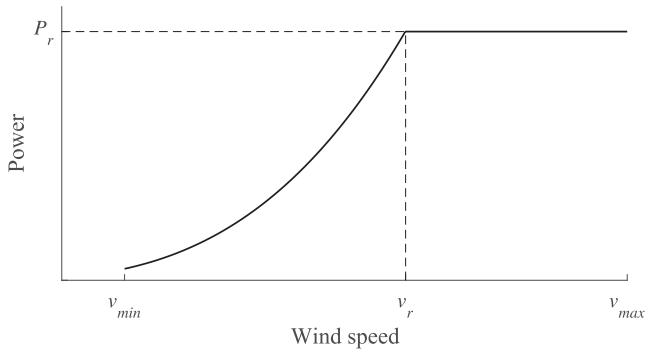


**Fig. 3.** Available power − wind speed $v$ characteristic.

Despite of the complexity of the aerodynamic interactions between turbines, suitable estimations can be achieved by modeling the wind speed deficit as a function of the geographical positions of the wind turbines, the atmospheric wind conditions, and the control actions required for the turbines, which affect the induction factor $a_i$. Assuming the velocity deficit behind the upstream turbine modeled as a quasi-steady state model with a linear relation between the induction factor and the downstream inlet velocity [24,25], and no recovery of the wake is considered, the incoming wind speed for the downstream turbine is given by

$$v_j = v_i\left(1 - \delta v(x_{ji}, s_i, a_i)\right), \tag{6}$$

where $i \in \{1,\dots,N-1\}$, $j = i+1$, $s_i$ is the spanwise distance behind the $i$-th turbine while the velocity deficit is

$$\delta v(x_{ji}, s_i, a_i) = \begin{cases} 2a_i c_{ji} & \text{if } s_i \le \dfrac{2R + 2\kappa_r c_{i,j}}{2} \\ 0 & \text{otherwise,} \end{cases}$$

with the coupling parameter $c_{ji} = (2R/(2R + 2\kappa_r(x_i - x_j)))^2$ including the information about the wind turbine distance, being $x_i$ and $x_j$ the positions of the upstream and downstream turbines respectively, and the roughness coefficient $\kappa_r$ that defines the wake expansion when passing through a turbine.[1]

In light of the previous expressions, the wake effect may be modified by properly acting on the induction factors $a_i$ with the aim of attenuating the wind deficits and thus for instance maximizing the power reserve and the wind farm capability for providing frequency support.

## 3. Wind farm controller

The primary objective of the wind farm controller is to track a power demand profile set by the TSO. This goal can be achieved with different power contributions of each turbine. This leaves an additional degree of freedom that can be used to satisfy other requirements. In the literature, several dispatch functions have been proposed to ensure different goals. For example, a simple approach distributes the total power proportionally to the available power of each turbine [28], while other distributions minimize the structural loads with the aim of ensuring a long turbine lifetime [29,30]. Here, we propose a control strategy that uses this degree of freedom to maximize the power reserve.

Assuming that the power $P_{\text{dem}}$ demanded by the TSO is lower than the total available power $P_{\text{av,tot}}$, the objectives are to regulate the total generated power at $P_{\text{dem}}$ and maximize the total power reserve $P_{\text{res}}$. Being the power demand $P_{\text{dem}}$ a parameter set by the TSO, the maximization of power reserve implies maximizing the total available power $P_{\text{av,tot}}$.

The available power at each turbine $P_{\text{av},i}$ depends on an increasing function of the wind speed faced by the rotor $v_i$ (see Fig. 3). Therefore, the maximization of the total available power can be seen as maximizing

$$J = \sum_{i=2}^{N} v_i(\mathbf{P_r}), \tag{7}$$

where $\mathbf{P_r} = [P_{r,1},\dots,P_{r,N}]^T$, and $P_{\text{r},i}$ is the power generation set-point at $i$-th turbine imposed by the wind farm control.

Due to the propagation of the wake effect, the generation conditions of the upstream turbines will affect the wind speed experienced by downstream turbines only after a certain time interval $T_s$, being this the time needed by the air flow to travel from one turbine to another. Notice that $T_s$ can be approximated as

$$T_s = s_i/c^*, \tag{8}$$

where $c^* = 0.7v_\infty$ indicates the variation of the convection velocity from the bottom to the top of the rotor disk [31], $v_\infty$ the free-stream wind speed and $s_i$ the distance between turbines.

Assume the wind turbines are evenly spaced and the set of turbine indices

$$\mathcal{N} = \{i : 1 \le i \le N \text{ and } v_i \ge v_j, \text{ for } i<j\}$$

is sorted according to the farm layout and dominant free-stream speed direction. That is, $i = 1$ corresponds to the turbine facing the free-stream speed ($v_\infty$) and $i = N$ the last one, facing the wind speed after passing through the entire farm. Hence, the value of the coupling parameter $c_{j,i}$ in (6) can be replaced by the constant $\kappa_2$. Therefore, defining $t = kT_s$ with $k \in \mathbb{Z}_{\ge 0}$, or simply $k$, the wind speeds faced by each turbine can be modeled as

$$\begin{aligned} v_1(k+1) &= v_\infty \\ v_2(k+1) &= v_1(k)(1 - \kappa_2 a_1(k)), \\ v_3(k+1) &= v_2(k)(1 - \kappa_2 a_2(k)), \\ &\vdots \\ v_N(k+1) &= v_{N-1}(k)(1 - \kappa_2 a_{N-1}(k)), \end{aligned} \tag{9}$$

with

$$v_\infty(k) = v_1(k) \ge v_2(k) \ge v_3(k) \ge \dots \ge v_N(k). \tag{10}$$

The induction factor $a_i$ is given by $P_{\text{r},i}$ according to (3). It can be seen from (3) that for a given $v_i$ an increase in $P_{\text{r},i}$ leads to an increase in $a_i$. From (9), this results in a higher wind speed deficit. Therefore, a heuristic approach to maximize (7) may be to minimize the power contributions of first wind turbines and maximize the contributions of the last ones (sorted according to $\mathcal{N}$). Keeping this idea in mind, in this work is proposed to compute the power set-point $P_{\text{r},i}$ for each wind turbine by solving the following linear programming problem:

[1] It is worth to mention that in Refs. [19,26] it has been shown that the previous wind speed formulation estimates a lower bound on the wind velocity in the wake. Recently, more efficient engineering wake models have been proposed to accurately estimate the impact of changes in induction factors on turbulence intensity generation and wake propagation, which affect how the wake expands and the effect of wind turbine generation of the wake recovery [27].

$$\underset{P_{r,i},\varepsilon}{\text{minimize}} \quad w^T\varepsilon \tag{11a}$$

$$\text{subject to} \quad P_{\text{dem}} = \sum_{i=1}^{N} P_{r,i}, \tag{11b}$$

$$\left| P_{\text{dem}} - \sum_{j=i}^{N} P_{r,j} \right| \leq \varepsilon_i, \quad i \in \mathcal{N}, \tag{11c}$$

$$P_{\min,i} \leq P_{r,i} \leq P_{\text{av},i}, \quad i \in \mathcal{N}, \tag{11d}$$

where $\varepsilon = [\varepsilon_1, \ldots, \varepsilon_N]^T$, $w = [w_1, \ldots, w_N]^T$ are weights such that $w_1 < w_2 < \ldots < w_N$, and $P_{\min,i}$ is the minimum power contribution.

Notice that constraint (11b) can be satisfied with multiple linear combinations of $P_{r,i}$. The optimization problem (11) seeks to find the combination with higher power contribution from the last group of turbines. In particular, with the selection of weights $w$ and the constraint (11c), the optimization problem can be seen as

try first $P_{r,N} = P_{\text{dem}}$,
if $P_{r,N} > P_{\text{av},N}$ then try $P_{r,N-1} = P_{\text{dem}} - P_{r,N}$,
if $P_{r,N-1} > P_{\text{av},N-1}$ then try $P_{r,N-2} = P_{\text{dem}} - P_{r,N} - P_{r,N-1}$,
and so on, until (11b) is satisfied.

In fact, if the lower limit $P_{\min}$ is removed, the problem can be solve algorithmically. Nevertheless, the lower limit is useful to prevent the shutdown of some turbines in high wind conditions.

The optimization problem (11) is solved at every time $T < T_s$ to produce a set of power references $P_{r,i}$, $i \in \mathcal{N}$. The application of these references alters the induction factors and thus the wake effect. As the proposed control strategy reduces the power contribution from the first set of turbines, the wind speeds faced by the last turbines increase resulting in higher available powers. As will be shown in the case study, after a few iterations this control strategy is able to increase the available power in the last turbines and then in the total power reserve.

As mentioned in the introduction, a decrease in the generation of the first turbines might also help to reduce mechanical loads and thus extending the lifetime of the wind farm [18,19]. However, the evaluation of loads is out of the scope of this paper.

## 4. Case study

### 4.1. Case description

The proposed control strategy was evaluated by simulation in the case of a wind farm with 12 benchmark NREL 5 MW wind turbines with radius of 63 m (a diameter $D = 126$ m). The wind turbines are evenly spaced along x- and y-directions by 630 m ($5D$). In order to consider the nonlinear nature of the wake propagation and the dynamic couplings among the turbines, the simulations were performed with the AEOLUS SimWindFarm (SWF) Simulink toolbox [32]. This tool, relatively simple compared with more detailed tools based on Large Eddy Simulations [26,31,33], uses the dynamic wake meandering model to estimate the wake effects according with the wind turbine layout and the ambient turbulence intensity.

The wind field size was $2500 \times 2500$ m$^2$ and the 2d (x,y) grid was spaced 15 m. Simulations were performed with laminar flow conditions, while the turbulence intensity was set equal to 0 to have a clearer view of the wind speed changes produced by the proposed strategy. Different wind directions were simulated by rotating the wind farm layout. Fig. 5 shows the wind fields $v_\infty = 11$ m/s with directions of 0 and 30° in steady-state conditions.

With the aim of evaluating the improvement in the power reserve, the proposed control algorithm was compared with the commonly used power distribution [22,32] established as

$$P_{r,i} = \min\left(\frac{P_{\text{dem}}}{P_{\text{av,tot}}} P_{\text{av},i}, P_{\text{av},i}\right), \quad i = 1, \ldots N. \tag{12}$$

### 4.2. Simulation results

#### 4.2.1. Scenario 1: low power demand and zero degrees wind speed direction

First, it is analyzed the system response when the power required by the TSO is set at 20 MW and the free-stream wind speed is 11 m/s with a direction of 0°. Fig. 6 shows the total values of the available power $P_{\text{av,tot}}$ (red line), the power demand $P_{\text{dem}}$ (dashed line), the power generated $P_g$ (blue line), and the power reserve $P_{\text{res}}$ (black line). Initially, for $t < 200$ s (shadow area), the wind farm controller sets the power set-points of each turbine according to the baseline power distribution (12). After $t = 200$ s, the controller starts computing the power set-points with the proposed control strategy (11). It can be observed in Fig. 6 that such strategy ensures the regulation of $P_g$ around the constant set-point $P_{\text{dem}} = 20$ MW during the whole simulation. On the other hand, it can also be seen that when the proposed control strategy is applied ($t \geq 200$ s), the available power $P_{\text{av,tot}}$ increases from 48 to 51 MW after a few steps. This represents (according to (1)) an increase in the power reserve $P_{\text{res}}$ from 28 to 31 MW. The new steady-state value is reached after 200 s.

Fig. 7 shows the power available $P_{\text{av},i}$ (red line), the power set-points $P_{r,i}$ (dashed line) and the power generated $P_{g,i}$ (blue line) for each wind turbine. The wind speed experienced by each turbine is shown in Fig. 8. The shadow areas in both figures correspond to the use of the baseline power distribution (12) ($t < 200$ s), in the analyzed scenario $P_{\text{dem}}/P_{\text{av,tot}} = 0.47$. In Fig. 8, it can be observed the wind speed deficit caused by the wake effect. With the baseline distribution, each turbine must contribute with 47% of its available power. The turbines in the first column are facing the free-stream speed 11 m/s, whereas the ones in the last column are experienced 10.23 m/s. As a result, the available power $P_{\text{av,i}}$ decreases from 5 MW in the first column (WT1, WT5, WT9) up to 3.71 MW in the last column (WT4, WT8, WT12).

When the proposed control strategy is applied at $t = 200$ s, the power set-points of the turbines in last column are set at the their available power. As a consequence of the larger contribution from these turbines, the remaining turbines reduce the power generation until the minimum value $P_{\min,i} = 1$ MW. As explained in Section 3, this reduction of the power generation in the turbines of the first columns implies a decrease of their induction factors and of the wind speed deficit in downstream turbines. These changes take about $T_s = 60$ s to reach the last column ($t_1 \simeq 260$ s) for the current case. This is the time needed by the wakes to travel through the columns. At $t = t_1$, the reduction in $P_{g,i}$ only affects the wind speeds faced by the turbines in the adjacent downstream column. The wind speed $v_i$ in Fig. 8 increases with respect to the initial conditions ($t < 200$ s) in 1.5% for turbines WT2, WT6, WT10, in 1.3% for WT3, WT7, WT11 and 1.2% for the last column. The increase in the wind speed faced by the downstream turbines causes an additional increase of the available power in the last column. As a result, the control strategy imposes a higher set-point to WT8 and WT4. The contribution of WT12 is now lower because the total available

power is enough to reach the power demand. This new distribution causes a new increase in the wind speed and thus in the available power until an equilibrium is reached after three steps, i.e., at $t_3 = 200 + 3T_s$ s.

Figs. 6–8 show that the proposed algorithm is able to reduce the wake effects and thus improves both the overall available power and the total power reserve.

*4.2.2. Scenario 2: low power demand and different wind directions*

For a more complete evaluation of the proposed strategy towards power reserve maximization, the control system was simulated under low power demand $P_{dem} = 20$ MW for different wind speed directions. Fig. 9 shows the power reserve for a free-stream wind speed $v_\infty = 11$ m/s with directions of 0, 20, 40, 60, 80, 90°. As in the previous case, the baseline control is used for $t < 200$ s, then the new power distribution algorithm is applied. In Fig. 9, it can be seen that the proposed strategy increases the power reserve for all wind directions compared with the baseline case. As mentioned in the previous section, the proposed algorithm needs several steps before reaching the equilibrium and these step times are affected by the time required from the wakes to travel through the wind farm columns. This propagation time is different for each direction because the distance the air flow must travel depends on the wind speed direction. Notice that higher improvements in $P_{res}$ are obtained when the wind turbines are totally in the wakes of the upstream turbines (see Figs. 4 and 5). As a result, the higher improvement occurs for both 0 and 90°, namely when the wind direction is perpendicular to x- or y- directions. Under these circumstances, $P_{res}$ increases from 28 MW for $t < 200$ s to 30.5 MW for $t > 500$ s when the direction of the wind is 0° and from 30 MW to 31.8 MW when the direction is 90°. If the turbines are only partially affected by the wakes, as the cases for 20, 40, 60 and 80°, the additional power reserve obtained with the proposed control strategy is low but the approach is still advantageous. For example, the difference between $P_{res}$ for $t < 200$ s and $t > 500$ s is about 0.4 MW at 20 and 60°, 0.92 MW and 1.4 MW for both 40 and 80°, respectively.

Fig. 10 presents the power reserve increments obtained with the proposed control strategy compared with the baseline expression, i.e., $\Delta P_{res} = P_{res,new} - P_{res,base}$, where $P_{res,new}$ is the reserve at $t > 500$ and $P_{res,base}$ is the power at $t = 0$. In this figure, three free-stream speeds, 11, 13, 15 m/s, were considered for several wind directions. Clearly, the proposed control achieves the highest improvement for $v_\infty = 11$ m/s. Under these circumstances, the total available power in the farm is close to the power demand and a clever distribution of the power contribution from each turbine makes a significant impact over the power reserve. In this case, the maximum $\Delta P_{res}$ is 2.36 MW at 0°, while lower differences are obtained for high wind speed conditions. Comparing different wind speed directions, it can be observed that the proposed control strategy produces higher improvements in the reserve for those

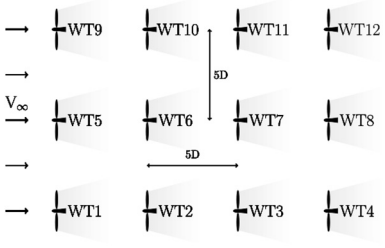


**Fig. 4.** Wind farm layout corresponding to the case study. The turbines are considered oriented to the free-stream wind speed direction.

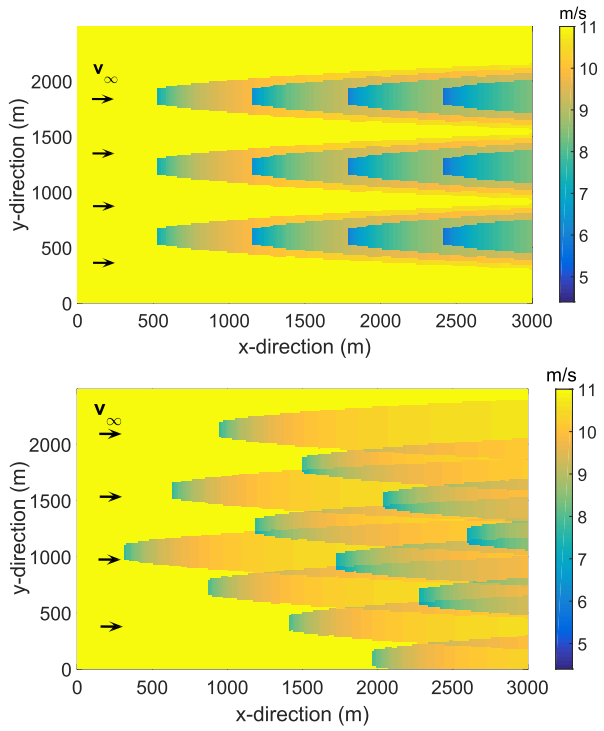


**Fig. 5.** Wind fields simulated with SWF for a wind farm of 12 turbines facing a $v_\infty = 11$ m/s. Top plot: wind field for a direction of 0°. Bottom plot: wind field for a direction of 30°.

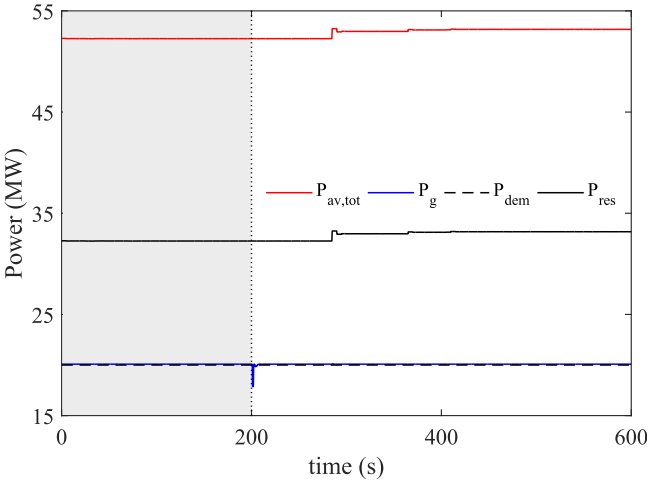


**Fig. 6.** Scenario 1: Power evolution for $v_\infty = 11$ m/s with a direction of 0°.

cases with higher air flow disturbances caused by the wakes. In particular, the lower reserve increment for the case of 90° compared with the 0° case can be understood as a consequence of the wind farm layout. When the wind speed reaches the farm with 90°, there are less turbines downstream and thus a lower wake effect. For the higher free-stream wind speed (13 and 15 m/s), the increase in the power reserve is lower because the available power is higher and the ratio $P_{dem}/P_{av,tot}$ is lower. As a consequence, the power required to the first column of turbines is lower and the wake effect less marked.

*4.2.3. Scenario 3: high power demand and different wind directions*

In Fig. 11, it can be observed the power reserve in case of a high

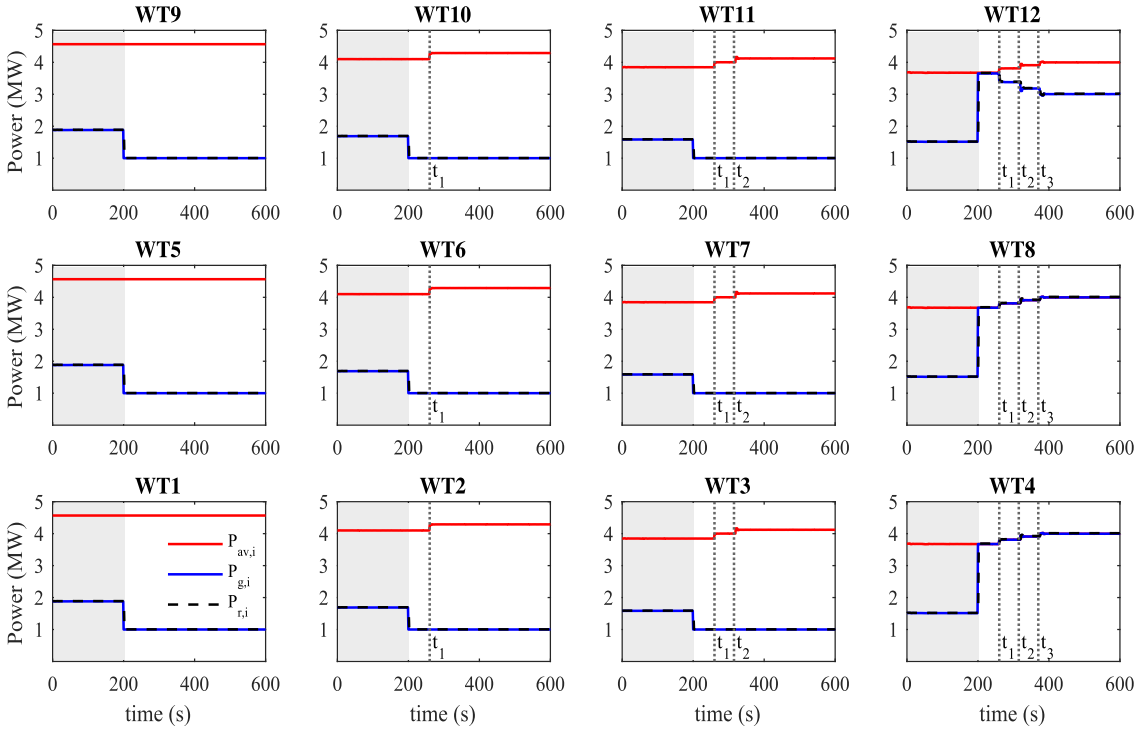


**Fig. 7.** Scenario 1: generated ($P_{g,i}$), available ($P_{av,i}$) and set-point ($P_{r,i}$) powers for each wind turbine. Shadow area: baseline power distribution function. White area: proposed distribution algorithm.

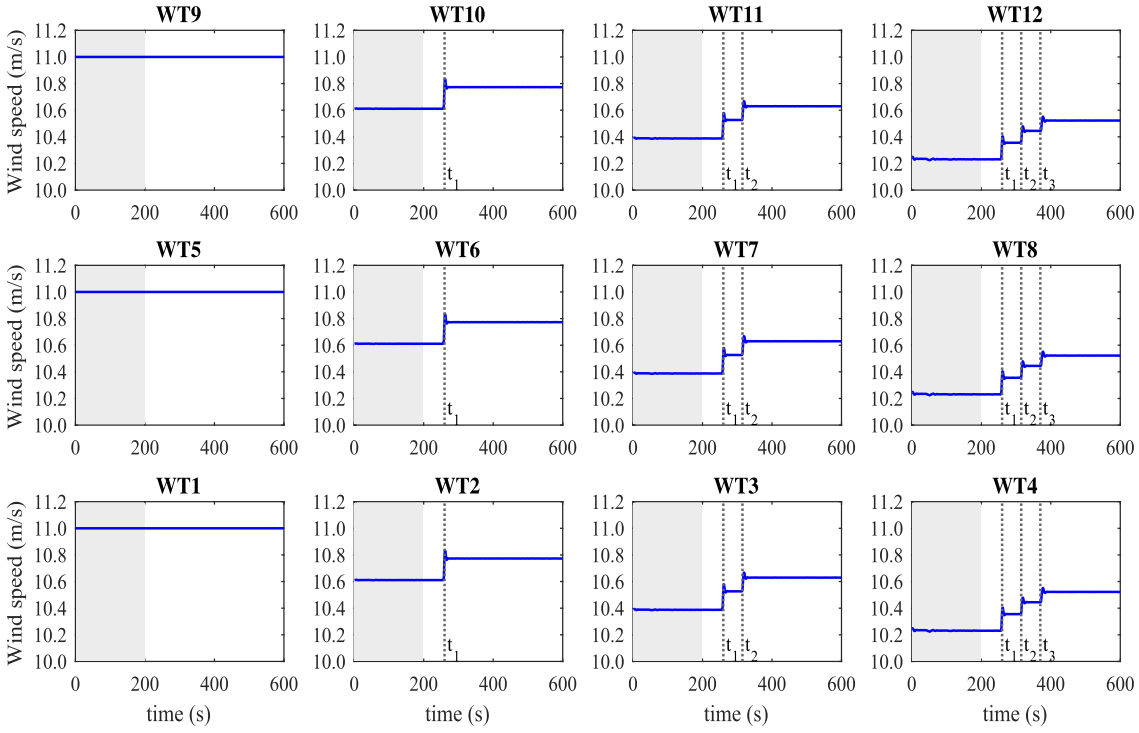


**Fig. 8.** Scenario 1: wind speeds faced by each turbine. Shadow area: baseline power distribution function. White area: proposed distribution algorithm.

power demand scenario. The power demand was $P_{dem} = 45$ MW and the free-stream wind speed $v_\infty = 11$ m/s, with directions of 0, 20, 40, 60, 80, 90°. Under these wind conditions, the available power is not enough to ensure the power demand. As a result, the reserve is almost zero except for the cases of 20, 40 and 60°, in which the wake effect has less impact on the available power. Nevertheless, the proposed approach is able to increase $P_{res}$ with respect to the value obtained with the baseline power distribution in 1.05 MW for 20°, in 1.6 MW for 60° and in 0.8 MW for 40° .

Fig. 12 presents the corresponding reserve increments $\Delta P_{res}$ for

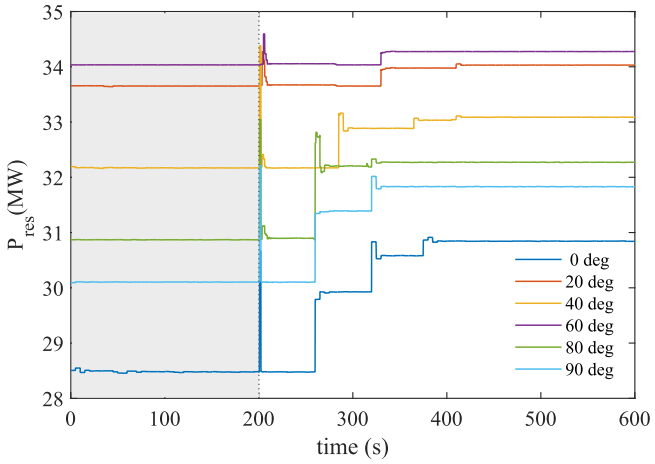


**Fig. 9.** Scenario 2: power reserve for several wind directions, $P_{dem} = 20$ MW, $v_\infty = 11$ m/s.

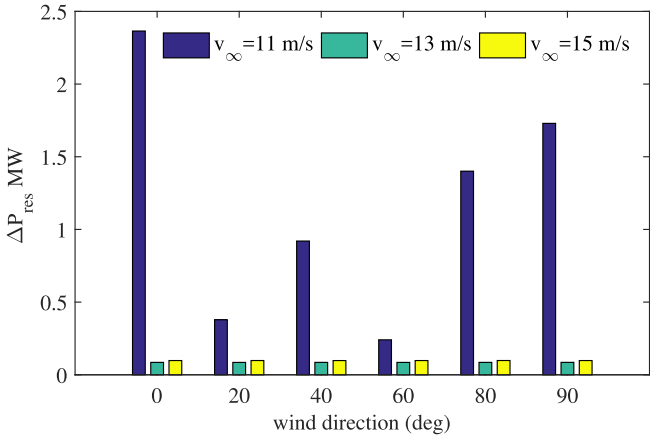


**Fig. 10.** Scenario 2: Summary of power reserve levels obtained with the proposed algorithm for several free-stream wind speeds and directions.

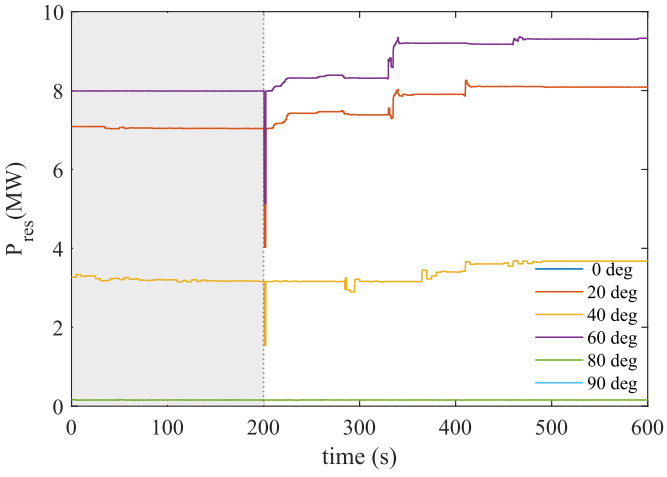


**Fig. 11.** Scenario 3: power reserve for several wind directions, $P_{dem} = 45$ MW, $v_\infty = 11$ m/s.

three free-stream wind speeds 11, 13, 15 m/s with the directions aforementioned. As the power demand is high and the available power is low in the case of 11 m/s, the improvement is only

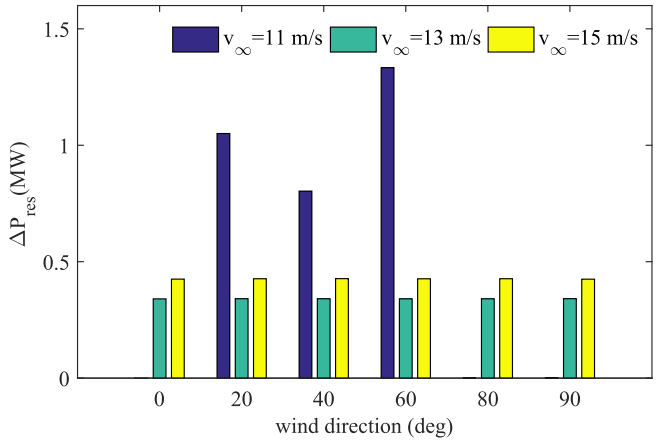


**Fig. 12.** Scenario 3: Summary of power reserve levels obtained with the proposed algorithm for several free-stream wind speeds and directions.

significant for the case in which the available power is higher than zero. On the other hand, when the wind speed is higher (13 and 15 m/s), the benefits of the proposed control strategy is more noticeable for all the wind directions as a result of higher wind power resources.

## 5. Conclusions

This paper has proposed a new control strategy to maximize the power reserve in WPPs while the power demanded by the TSO is satisfied. The proposed approach seeks to distribute the power contribution of each turbine in order to reduce the wind speed deficits caused by wake effects. The idea is to prioritize the power contribution of the most downstream turbines and thus attenuating the wake disturbances. The proposed strategy was evaluated by simulation in the case of 12 turbine WPP under different scenarios, including low and high power demands and several wind speed conditions. The results show that the control strategy is capable of increasing the power reserve compared with the conventional power distribution where the power set-points of each wind turbine are proportional to its available power. The best performance is obtained when the power demanded by the TSO is close to the total available power. In these cases, a clever distribution of the power contributions from each turbine reduces the negative effects of wakes and produces a significant increase in the power reserve compared to the conventional approach. Left as future research to evaluate the performance of the proposed algorithm in high fidelity wind farm models. Another point to further study is the possible beneficial effects of the propose redistribution of the power contribution on the mechanical load and thus in the lifetime of the wind farm.

## Acknowledgments

This work has received funding from the European Union's Horizon 2020 research and innovation programme under the Marie Skodowska-Curie grant agreement No 675318 (INCITE).

## References

[1] WindEurope, Wind Energy in Europe, Scenarios for 2030, Sep. 2017. https://windeurope.org/about-wind/reports.
[2] V. Gevorgian, Y. Zhang, E. Ela, Investigating the impacts of wind generation participation in interconnection frequency response, IEEE Trans. Sustain. Energy 6 (3) (2015) 1004–1012.
[3] S. Boersma, B. Doekemeijer, P. Gebraad, P. Fleming, J. Annoni, A. Scholbrock,

J. Frederik, J. van Wingerden, A tutorial on control-oriented modeling and control of wind farms, in: Proc. of American Control Conference (ACC), 2017, pp. 1–18.
[4] J.M. Mauricio, A. Marano, A. Gómez-Expósito, J.L.M. Ramos, Frequency regulation contribution through variable-speed wind energy conversion systems, IEEE Trans. Power Syst. 24 (1) (2009) 173–180.
[5] A. Tapia, G. Tapia, J. Ostolaza, Reactive power control of wind farms for voltage control applications, Renew. Energy 29 (3) (2004) 377–392.
[6] S. Ataee, H. Bevrani, Improvement of primary frequency control by inertial response coordination between wind and conventional power plants, Int. Trans. Electr. Energy Syst. 27 (8) (2017) 235–245.
[7] S. De Rijcke, J. Driesen, J. Meyers, Power smoothing in large wind farms using optimal control of rotating kinetic energy reserves, Wind Energy 18 (10) (2015) 1777–1791.
[8] A. De Paola, D. Angeli, G. Strbac, Scheduling of wind farms for optimal frequency response and energy recovery, IEEE Trans. Control Syst. Technol. 24 (5) (2016) 1764–1778.
[9] EWEA, Balancing responsibility and costs of wind power plants. https://www.ewea.org/fileadmin/files/library/publications/position-papers/EWEA-position-paper-balancing-responsibility-and-costs, 2015.
[10] T.G. Bozkurt, G. Giebel, N.K. Poulsen, M. Mirzaei, Wind speed estimation and parametrization of wake models for down regulated offshore wind farms within the scope of PossPow project, in: Journal of Physics: Conference Series vol. 524, IOP Publishing, 2014, p. 012156.
[11] S. Frandsen, R. Barthelmie, S. Pryor, O. Rathmann, S. Larsen, J. Højstrup, M. Thøgersen, Analytical modelling of wind speed deficit in large offshore wind farms, Wind Energy 9 (1–2) (2006) 39–53.
[12] P. Gebraad, F. Teeuwisse, J. Wingerden, P.A. Fleming, S. Ruben, J. Marden, L. Pao, Wind plant power optimization through yaw control using a parametric model for wake effects: a CFD simulation study, Wind Energy 19 (1) (2016) 95–114.
[13] J. Park, K.H. Law, Layout optimization for maximizing wind farm power production using sequential convex programming, Appl. Energy 151 (2015) 320–334.
[14] J. Annoni, A. Scholbrock, M. Churchfield, P. Fleming, Evaluating tilt for wind farms (i), in: Proc.. of American Control Conference (ACC), 2017, pp. 717–722.
[15] M. Vali, J. van Wingerden, S. Boersma, V. Petrović, M. Kühn, A predictive control framework for optimal energy extraction of wind farms, in: Journal of Physics: Conference Series vol. 753, IOP Publishing, 2016.
[16] S. Siniscalchi Minna, F. Bianchi, C. Ocampo Martinez, Predictive control of wind farms based on lexicographic minimizers for power reserve maximization, in: Proc. of American Control Conference (ACC), IEEE, 2018, pp. 701–706.
[17] S. Siniscalchi-Minna, M. De-Prada-Gil, F. Bianchi, C. Ocampo-Martinez, B. De Schutter, A multi-objective predictive control strategy for enhancing primary frequency support with wind farms, in: Journal of Physics: Conference Series vol. 1037, IOP Publishing, 2018, p. 032034.
[18] T.N. Jensen, T. Knudsen, T. Bak, Fatigue minimising power reference control of a de-rated wind farm, in: Journal of Physics: Conference Series vol. 753, IOP Publishing, 2016, p. 052022.
[19] F. Campagnolo, V. Petrović, C.L. Bottasso, A. Croce, Wind tunnel testing of wake control strategies, in: American Control Conference, IEEE, 2016, pp. 513–518.
[20] G.C. Larsen, H. Madsen Aagaard, F. Bingöl, J. Mann, S. Ott, J.N. Sørensen, V. Okulov, N. Troldborg, N.M. Nielsen, K. Thomsen, et al., Dynamic Wake Meandering Modeling, Tech. rep., Risø National Laboratory, 2007.
[21] J.F. Manwell, J.G. McGowan, A.L. Rogers, Wind Energy Explained: Theory, Design and Application, John Wiley & Sons, 2010.
[22] L. Holdsworth, J.B. Ekanayake, N. Jenkins, Power system frequency response from fixed speed and doubly fed induction generator-based wind turbines, Wind Energy 7 (1) (2004) 21–35.
[23] A. Zertek, G. Verbic, M. Pantos, A novel strategy for variable-speed wind turbines' participation in primary frequency control, IEEE Trans. Sustain. Energy 3 (4) (2012) 791–799.
[24] N.O. Jensen, A Note on Wind Generator Interaction, Tech. rep., Roskilde, Denmark, 1983.
[25] E. Bitar, P. Seiler, Coordinated control of a wind turbine array for power maximization, in: Proc. of American Control Conference (ACC), IEEE, 2013, pp. 2898–2904.
[26] J. Annoni, P.M. Gebraad, A.K. Scholbrock, P.A. Fleming, J.-W. v. Wingerden, Analysis of axial-induction-based wind plant control using an engineering and a high-order wind plant model, Wind Energy 19 (6) (2016) 1135–1150.
[27] M. Bastankhah, F. Porté-Agel, Experimental and theoretical study of wind turbine wakes in yawed conditions, J. Fluid Mech. 806 (2016) 506–541.
[28] A.D. Hansen, P. Sørensen, F. Iov, F. Blaabjerg, Centralised power control of wind farm with doubly fed induction generators, Renew. Energy 31 (7) (2006) 935–951.
[29] P. Fleming, J. Aho, P. Gebraad, L. Pao, Y. Zhang, Computational fluid dynamics simulation study of active power control in wind plants, in: Proc. of American Control Conference (ACC), 2016, pp. 1413–1420.
[30] H. Zhao, Q. Wu, Q. Guo, H. Sun, Y. Xue, Distributed model predictive control of a wind farm for optimal active power control, part II: implementation with clustering-based piece-wise affine wind turbine model, IEEE Trans. Sustain. Energy 6 (3) (2015) 840–849.
[31] U. Ciri, M.A. Rotea, S. Leonardi, Model-free control of wind farms: a comparative study between individual and coordinated extremum seeking, Renew. Energy 113 (2017) 1033–1045.
[32] J.D. Grunnet, M. Soltani, T. Knudsen, M.N. Kragelund, T. Bak, Aeolus toolbox for dynamics wind farm model, simulation and control, in: The European Wind Energy Conference & Exhibition, EWEC, 2010.
[33] C. Santoni, K. Carrasquillo, I. Arenas-Navarro, S. Leonardi, Effect of tower and nacelle on the flow past a wind turbine, Wind Energy 20 (12) (2017) 1927–1939.